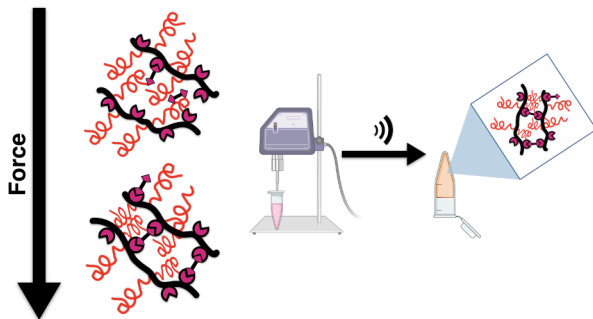


Molecularly Shielded, On-Demand, Ultrasound-Cured Polymer Networks

Adrian A. Lorenzana¹, Hsu Shwe Yee Naing¹, Jichao Song¹, Jessica D. Schiffman¹, John Klier², Shelly R. Peyton¹

¹Department of Chemical Engineering, University of Massachusetts Amherst, Amherst, Massachusetts 01003, United



States

²Department of Chemical Engineering, Oklahoma University, Norman, Oklahoma 73019, United States

Abstract: Networks formed from polymers can range from soft hydrogels to ultrahard protective coatings, making them useful for a wide range of applications from cell culture to highly bonded adhesives. Polymer networks are commonly crosslinked *via* heat or high energy light, and recently mechanical force has also been used to induce the formation of crosslinks in pre-existing networks. Here, we demonstrate a new strategy to use mechanical deformation and ultrasound to induce liquid-to-solid crosslinking. We synthesized graft copolymers with large poly(ethylene glycol) (PEG) side-chains acting as molecular shielding groups to protect otherwise highly reactive epoxide group. Solutions of highly shielded polymers could remain as a liquid solution when left undisturbed, and we could initiate gelation of these solutions with ultrasound in 20 seconds. These ultrasound-sensitive polymers are particularly useful in light and heat sensitive applications, and where precise control over the gelation time is required.

Keywords: Epoxide, poly(ethylene glycol), methacrylates

Introduction

Polymer networks can be crosslinked *via* permanent covalent bonds. Polymer networks can include super-soft hydrogels that mimic human tissue¹, protective ultra-hard coatings², and highly bonded adhesives³. Highly crosslinked lightweight networks, such as those formed with epoxide, are crucial in industrial applications like transportation, where reducing vehicle weight improves passenger safety and reduces harmful greenhouse gas emissions. The process of crosslinking or “curing” polymers is typically accomplished *via* a) mixing, b) heat, c) high energy light, or d) electron beams⁴. Heat and light are popular routes, as they facilitate curing on-demand, allowing liquid application to a substrate. However, light and heat are not always feasible, as light cannot pass through opaque materials, and heat can damage delicate or flammable substrates. Electron beams are also popular industrially due to their high energy efficiency and excellent uniformity, however transmittance through metals can be challenging.

Alternatively, natural polymers (e.g. peptides, saccharides, nucleic acids), can form networks in response to temperature, light, and solvents by partially unfolding, thus exposing previously buried, or “cryptic”, binding sites. Of particular interest to us, these cryptic binding sites can also be revealed in response to a mechanical stimulus^{5,6}. For

example, fibronectin will dynamically unfold and polymerize into fibrils in response to cell-generated forces⁷⁻⁹. In contrast, synthetic polymers commonly weaken or even rupture under force¹⁰.

Inspired by the unfolding triggered crosslinking of proteins like fibronectin, we sought to develop a new method of installing mechanosensitivity within synthetic polymer networks. Recently, we developed organogels¹¹ and hydrogels¹² with mechano-responsive properties, both based on preformed diacrylate crosslinks with reactive pendent thiols for post-polymerization crosslinking. Both systems begin as a crosslinked network and respond to compression, strengthening several hundreds of kPa in elastic modulus over repeated cycles. The mechanosensitivity results from long PEG molecular shielding groups grafted to the polymer backbone, which prevent the reactive thiol groups from crosslinking until compression brings them together.

To date, the most successful method of creating synthetic mechanosensitive polymers that undergo liquid-to-solid transition is by inserting weak bonds, “mechanophores,” within polymer chains that are converted to an active intermediate in response to force, capable of strengthening the material¹³⁻¹⁵. Still other approaches to designing force-sensitive materials involve the design of small molecules

with several ways of participating in intermolecular interactions such as hydrogen bonding, π - π stacking, and van der Waals forces. Peptide-based isomers functionalized with cholesterol and naphthalic groups have been shown to create micellar assemblies that undergo a gel-gel transition with the application of ultrasound¹⁶. This work, in contrast, uses the shielding group concept, starting with uncrosslinked, shielded polymers that can undergo a rapid liquid-to-solid transition upon application of force. To accomplish this, graft polymers bearing reactive epoxide¹⁷ groups are mixed with small molecule amine/thiol crosslinkers. Ultrasonic irradiation is used to apply high strain rates to the shielded polymers. Straining of the graft polymers overcomes their steric barrier to interaction with the small molecule crosslinkers, facilitating a reaction, that rapidly strengthens the material. The resultant materials achieve elastic modulus values comparable to ultra hard commercial epoxy coatings. We anticipate that these shielded polymers will be useful as extremely hard and solvent-resistant coatings and as adhesives that can be cured by focusing ultrasound through the surfaces the adhesive is bound to.

Materials and Methods

Chemicals and polymer sourcing

Materials were purchased from Sigma-Aldrich unless otherwise mentioned. Poly(ethylene glycol) methyl ether methacrylate (500 g/mol and 950 g/mol, PEGMA500 and PEGMA950 respectively), glycidyl methacrylate (97%, GMA), and 2-methoxyethyl methacrylate (99%, MEMA) were passed through a column of neutral alumina to remove inhibitors before use. 2,2'-(Ethylenedioxy)diethanethiol (95%, EDT), ethylene diamine (99%, EDA), 2-phenyl-2-propyl benzodithioate (99%, PPB), 4-cyano-4-(phenylcarbonothioylthio)pentanoic acid (98%, CPA), and 2-(azo(1-cyano-1-methylethyl))-2-methylpropane nitrile (98%, AIBN), 1-butanol (99.9%, BuOH), 1,4-dioxane (99%, dioxane), N,N-dimethylformamide (99.8%, DMF) were used as received. Diethyl ether (99%, ether), lithium hydroxide monohydrate (98.5%, LiOH), and acetonitrile (99%, MeCN) were purchased from Fisher Chemical and used as received. Basic alumina 60-325 mesh was purchased from Fisher Scientific and used as received.

Representative polymer synthesis

Poly(GMA-co-PEGMA) and poly(GMA-co-MEMA) of all molar ratios and degree of polymerization (DP) were synthesized by reversible addition-fragmentation chain transfer (RAFT) polymerization. The targeted monomer ratios and DP are described in **Table 1**. Each reaction was fed 0.01 moles of monomer total. For example, 0.71 g (0.005 mol) GMA, 0.72 g (0.005 mol) MEMA, 0.0559 g CPA (0.2 mmol), 6.6 mg AIBN (0.04 mmol) ([50]:[1]:[0.2] [M]:[CTA]:[I], where [M]:[CTA] defines the DP), 4 mL of 1,4-dioxane, and a stir bar were added to a 20 mL scintillation

vial. The vial was sealed with a rubber septum and the solution was purged with N₂ (g) for ~20-30 min in an ice bath to prevent solvent and monomer evaporation (PEGMA solutions were bubbled in cool water to prevent PEG crystallization). Subsequently, the vial was placed in a thermostated aluminum reaction block at 60 °C on top of a magnetic stir/hot plate. The reaction was left to stir overnight, yielding a viscous liquid. The solution was removed from heat and exposed to air to terminate the polymerization. The solution was precipitated into cold (-20 °C) ether, the solid washed twice more with cold ether, and dried at 0.01 mbar overnight.

Polymer characterization

Polymer DP and the comonomer incorporation ratio were determined through ¹H NMR on a Bruker Avance 500 at 500 MHz in CDCl₃ (Figures S1-10)¹⁸. The ratio of monomers was determined by integration of ¹H spectral resonances of the PEGMA/MEMA methoxy protons and the methanetriyl proton of the GMA glycidyl ring, normalized to the aromatic proton peak at the para position of the CPA phenyl ring, assuming there is one Z group¹⁹ on every polymer chain.

Copolymer solution preparation

Polymer solutions were initially prepared to be 50 wt% polymer. For example, 0.3 g of polymer was dissolved in 0.3 g of solvent, and crosslinker was added such that the nucleophilic functional group was equimolar with the total epoxide concentration. To control for the concentration of crosslinking points in solution, polymers were subsequently formulated to be 1 M of epoxide in solution. For copolymers containing PEGMA2000, solutions were formulated in MeCN at 0.5 M of epoxide functional units due to the large pendant chains dominating the overall mass of the sample and crosslinked with EDT catalyzed by LiOH. Each sample was vortexed for 5 sec to ensure complete mixing before proceeding with rheometry or sonication.

For all experiments crosslinked with amines, reactions were conducted in a solvent system of 1:1 BuOH:DMF. Alcohols are known to catalyze the reaction between amines and epoxides through the formation of a trimolecular complex²⁰. Thiol-crosslinked reactions were conducted in MeCN with 10 μ L of 2 M LiOH as a catalyst, necessary to deprotonate the thiols in order to perform a nucleophilic attack on the epoxide ring²¹.

Parallel plate rheology
Gelation times and storage moduli (G'), and $\tan\delta$ of polymer solutions/gels were determined on a Kinexus Pro parallel plate rheometer (Netzsch, Selb, Bayern, Germany). Measurements were run on a 20 mm plate with

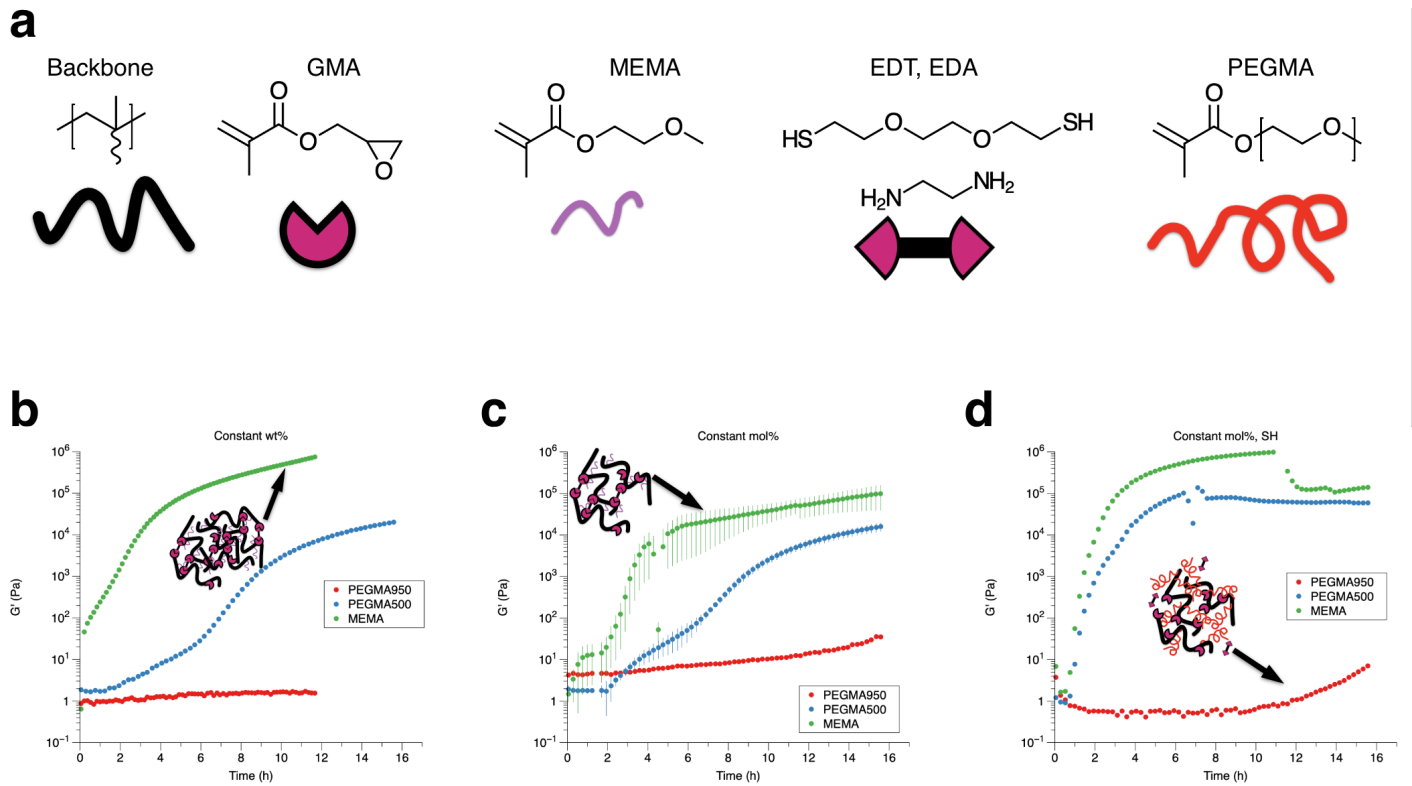


Figure 1. Large molecular shields inhibit or delay crosslinking. **a.** Illustrations of polymer components used throughout the paper. **b.** Effect of shielding group functionality on storage modulus (G') over time with amine crosslinks at constant 50 wt % polymer, reacting with EDA. Inset depicts high density poly(GMA-co-MEMA) with many epoxy groups. **c.** Effect of shielding group functionality on storage modulus over time with amine crosslinks at constant 1 M concentration epoxy, reacting with EDA. Inset depicts low density poly(GMA-co-MEMA) with a fixed amount of epoxy groups. **d.** Effect of shielding group functionality on storage modulus over time with thiol crosslinks at constant 1 M concentration epoxy, reacting with EDT. Inset depicts poly(GMA-co-PEGMA950) with a fixed amount of epoxy groups and large shielding groups preventing crosslinking. For all experiments, a 1:1 ratio of GMA:MEMA, PEGMA500, or PEGMA950 was used. Error bars show the standard deviation of G' at each timepoint ($n = 3$). For all conditions, including the enhanced kinetics provided by the thiol-epoxy reaction, a latency period before gelation at static conditions is present.

a 1 mm gap at 1% strain and 1 – 100 rad s^{-1} frequency sweep. Each frequency sweep lasted approximately 5 min, and the entire measurement lasted approximately 15 hr. The gel point was defined using the Winter-Chambon criterion, for which the time of gelation is defined as the point at which $\tan\delta$ becomes frequency independent at small frequencies²²⁻²⁴. For samples with very high modulus, the elastic modulus was determined using compressive rheology by taking the slope of the stress strain curve of cured gels with a 4 mm diameter. Rheological experiments were analyzed using IRIS Rheo-Hub (IRIS Development, Amherst, MA)²⁵.

Sonication-induced gelation of shielded copolymers

Polymer solutions were sonicated using a QSonica Q500 with a microtip attachment. The microtip QSonica probe was immersed in a polymer solution in MeCN. Water was flowed across the outer surface of the tube using a custom-made jacketed beaker to control bulk temperature (Video S1) (University of Massachusetts Amherst Scientific Glassblowing Laboratory, Amherst, MA). Temperature was monitored with an IRT205 IR thermometer (General Tools, Secaucus, NJ) and confirmed with a mercury

thermometer. This cooling setup was not sufficient to control temperature after 2 min and 40 s of sonication. Samples were sonicated at 10% amplitude and 20 kHz for 5 sec at a time, with 10 sec breaks in between pulses to avoid probe overheating. Gelation was determined by the point at which the power output would drop to ~0 W and noise from vibrations would cease when the polymer had formed a solid gel. Samples were then immediately moved to the adjacent needle induced cavitation (NIC) setup to determine the elastic modulus immediately post sonication.

Differential scanning calorimetry

Differential scanning calorimetry (DSC, Q200, TA Instruments) was used for crystallization characterization. A sample of (3-5 mg) was sealed in a standard aluminum hermetic pan using TZERO press (TA Instruments) before being added to the calorimeter with an identical empty reference pan. The equipment was lowered to -90 °C and heated to 100 °C at a rate of 5 °C/min to remove the thermal history of the sample. The equipment was then lowered to -90 °C again and heated to 100 °C at the same

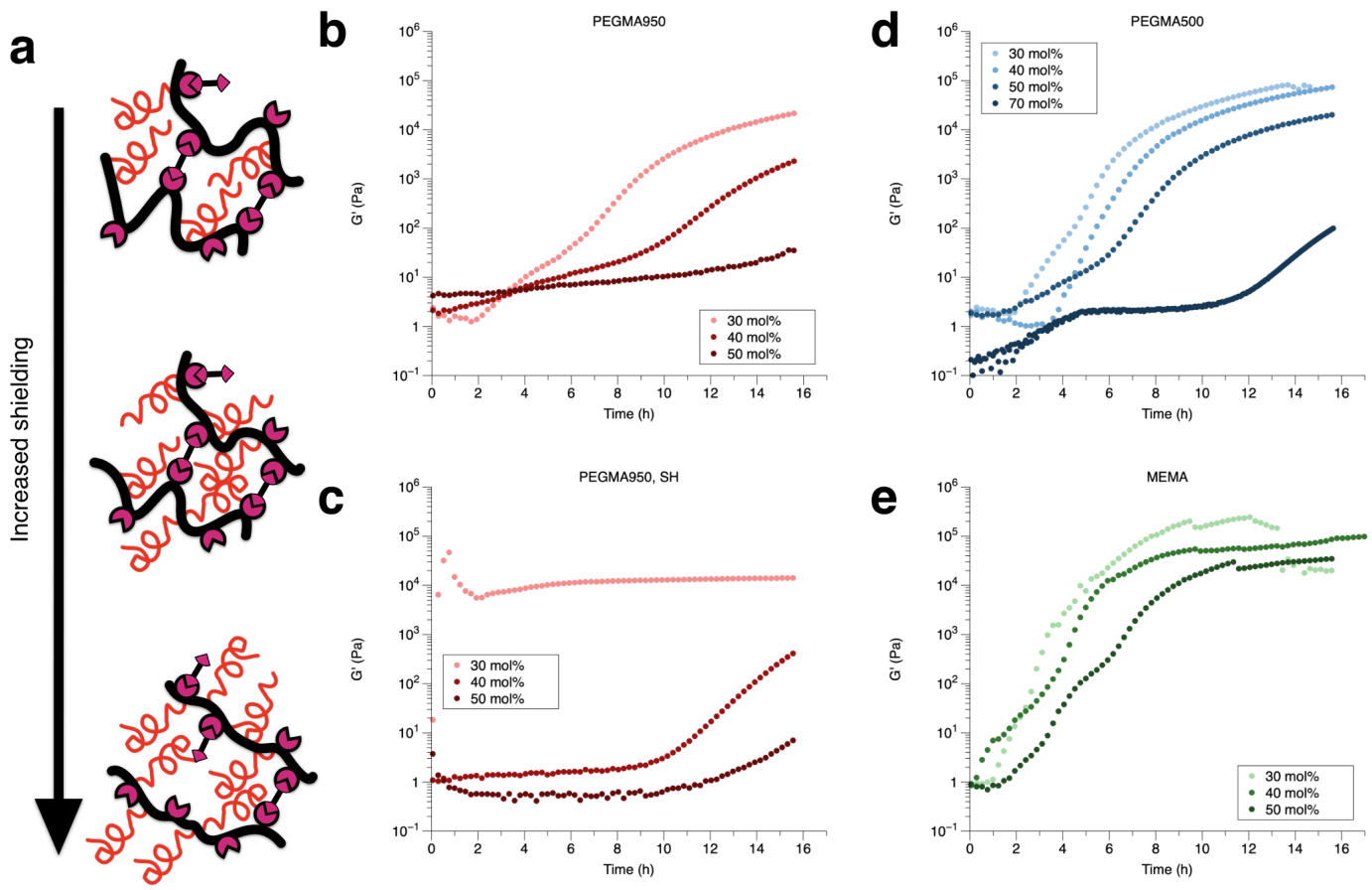


Figure 2. Ratio of pendent shields to reactive groups controls gelation time. **a.** Illustrations of polymers at different GMA:PEGMA molar ratios, showing the change in backbone flexibility and exposed reactive sites. **b-e.** Storage modulus evolution over time for: (**b-c**) varying mole percentage of PEGMA950 with a diamine (**b**) or dithiol (**c**) crosslinker; (**d**) varying mole percentage of PEGMA500 and (**e**) MEMA with a diamine crosslinker. Arrows represent trends in shielding resulting from increased ratio of shielding monomer.

rate, where enthalpy of melting (ΔH_m) was obtained from the area of the melting curve divided by the sample weight²⁶. Thermogravimetric analysis (TGA, Q50, TA Instruments) was used to determine the degradation of the samples before running DSC to meet the criteria of a maximum 1.5 wt% loss.

Needle induced cavitation

Characterization of elastic modulus of sonicated gels was done with needle induced cavitation (NIC) using a custom-made setup with water as the fluid, pressurized with a NE 1000 syringe pump (New Era, Farmingdale, NY), contained in a 6 mL disposable syringe with a 27-gauge stainless steel disposable needle, microstand, and Px409-015 GUSBH pressure gauge (Omega, Norwalk, CT). Data collected from NIC was recorded on a Surface Mini using a custom LabView program to interface with the pressure sensor and record the pressure values (Crosby Lab, University of Massachusetts Amherst, Amherst, MA). When calculating the elastic modulus of gels, the effects of surface tension were ignored and values were computed using **Equation 1**^{27,28}. Each NIC experiment lasted on average from 30-90 sec.

$$E = \frac{6P_c}{5} \quad (1)$$

Results and Discussion

Gelation kinetics of polymers under static conditions

Our goal was to create a polymer network that was shelf-stable and would gel in response to force. First, we created a suite of polymers with varying crosslinker to comonomer ratios. Shielded and control copolymers were synthesized using RAFT polymerization of PEGMA (molecular shielder, grafting-through process²⁹) or MEMA (control) with GMA monomers. Poly(GMA-*co*-PEGMA) and poly(GMA-*co*-MEMA) were synthesized with varying monomer ratios (30:70 GMA:PEGMA/MEMA to 70:30 GMA:PEGMA/MEMA) and shield lengths (1, ~10, and ~20 PEG repeats for MEMA, PEGMA500, and PEGMA950, respectively) to determine their effect on gelation. Additionally, DP for each composition was varied to determine the effect of polymer length on force sensitivity.

When developing these materials, we imagined a polymer system that would be easily spreadable onto a substrate as a liquid that would then transition to a solid state after

the introduction of mechanical stimuli. The final solid material should be bonded together permanently with covalent crosslinks. To achieve this goal, we selected the monomer GMA for its robust epoxide reactive group. Epoxides are known to undergo a ring-opening reaction in the presence of nucleophiles like amines and thiols. To introduce mechano-sensitivity, we sought to copolymerize our epoxide functional monomers with monomers functionalized with groups that could provide steric hindrance. Towards this goal, GMA was co-polymerized with PEGMA of varied molecular weights from 140 to 950 g/mol that we hypothesized could provide a steric hindrance to crosslinking via their ether side-chains.

Synthesis of this suite of polymers proceeded as expected, with final DPs and incorporation ratios closely matching the targeted DP and feed ratio when conducted in dioxane (**Table 1**). Successful incorporation and molar ratio of constituent monomers was confirmed using ^1H NMR spectroscopy (Figures S1-10). DP and incorporation ratios of poly(GMA-*co*-PEGMA) samples were less consistent compared to their MEMA counterparts, attributed to the inherent dispersity of PEGMA macromonomers skewing the actual molar amount added to reactions. After successfully synthesizing the desired copolymers, we moved on to assess their gelation kinetics.

For our crosslinkers, we chose EDT due to its non-volatile nature and reasonable stability in air, and EDA as it is commonly used to cure epoxy resins. Amines and thiols were chosen as two candidates both because they are frequently used in commercial epoxy formulations and to compare the effects of different reaction kinetics on the shielded copolymer system. We sought to determine a molecular weight of shielding groups that would facilitate delayed crosslinking of the epoxide groups in the presence of a bifunctional nucleophile without preventing it entirely. In our experiments, we tested a range of effects including varying the DP of grafted chains from 1 to 20, varying the DP of the polymer backbone from 25 to 670, adjusting nucleophilic attack kinetics, and varying the ratio of comonomers from 30 to 70% GMA concentration. The monomers used to form the copolymers and the different crosslinkers in these experiments are represented in **Figure 1a**.

First, the effect of pendent shield size on crosslinking was assessed at constant weight percent and static conditions (**Figure 1b**). When solutions are formulated at 50 wt% of polymer with EDA, poly(GMA-*co*-MEMA) crosslinks very quickly (1 h) and reaches a final G' on the order of 10^6 Pa. Conversely, poly(GMA-*co*-PEGMA500) crosslinks more slowly (8 h) and reaches a final G' on the order of 10^4 Pa, and poly(GMA-*co*-PEGMA950) shows no change in modulus indicating no crosslinking occurred. At constant 50 wt% of polymer in solution, the concentration of epoxide

for unshielded samples (MEMA) is very high compared to the shielded polymers (PEGMA). At this fixed concentration, the overall mass for the shielded polymer solutions is dominated by the presence of ether in the PEGMA side chains, skewing the sample in favor of unreactive ether and decreasing the number of possible crosslinks. The lack of increase in modulus with PEGMA950 may be due to this ether dominance preventing the formation of a volume-spanning network. Additionally, the relatively large mass of the ether side-chains decreases the amount of reactive epoxy in solution.

To control for the effect of variable epoxide concentration, samples were next formulated at a constant epoxide molar concentration (**Figure 1c**). Epoxide concentration was set to 1 M, resulting in variable weight percent polymer in solution: control polymer samples with low (25%) and shielded samples with high (61%) weight percent. At 25 wt%, poly(GMA-*co*-MEMA) crosslinks more slowly (2 h) than at 50 wt% and reaches a lower final G' on the order of 10^5 Pa. For poly(GMA-*co*-PEGMA950), wt% changes from 50 to 61 and expectedly shows only a small increase in G' of 35 Pa. For poly(GMA-*co*-PEGMA500 samples, 1 M epoxide concentration is equal to 50 wt% of polymer. Trends in the effect of shielding groups are the same at constant wt% polymer or mol% epoxides: as the shielding group MW increases, the time to gelation and the final

Table 1. Polymers used in each experiment, their target DP, comonomer feed ratio, actual DP, and actual comonomer ratio as determined by ^1H NMR modulus both decrease.

Finally, the effect of more reactive nucleophiles on crosslinking were investigated by replacing EDA with EDT and keeping the mol% epoxide constant (**Figure 1d**). Thiols are known to be stronger nucleophiles than primary amines, and the ring opening reaction between thiols and epoxides proceeds orders of magnitude faster than between amines and epoxides³⁰. At a constant 1 M epoxide concentration, poly(GMA-*co*-MEMA) with EDT crosslinked more rapidly (30 min) than the amine condition and attained a similar final G' . Poly(GMA-*co*-PEGMA500) samples crosslinked rapidly (42 min) with EDT, but more slowly than the MEMA copolymer and attained a final modulus on the order of 10^4 Pa. Poly(GMA-*co*-PEGMA950) samples still did not show any signs of gelation, increasing only to a final modulus of 10 Pa. Even with faster reaction kinetics, the PEGMA950 shielding groups suppress gelation.

For permanently crosslinked polymer networks, the equilibrium modulus of the cured material can be predicted by Flory's theory of rubber elasticity^{31,32} and is proportional to the number of elastically effective chains in the network^{33,34}. As the number of elastically effective chains increases, so does the equilibrium modulus; therefore, a

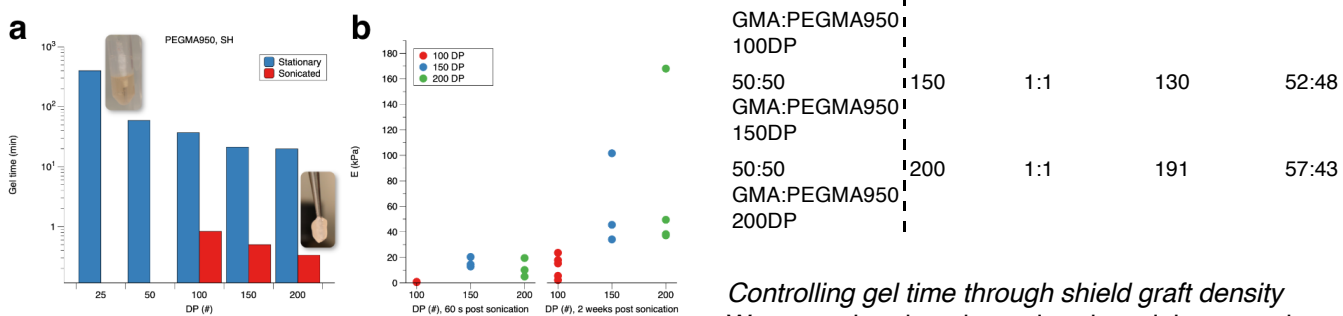


Figure 3. Sonication induces shielded polymer crosslinking. **a.** Gel time of poly(GMA-*co*-PEGMA950) under static and sonicated conditions at varying DP with 1:1 molar ratio. Samples at 25 and 50 DP did not form a gel. Insets show a liquid polymer solution during a bubble test and a polymer cured through sonication, still attached to the sonicator probe. **b.** Elastic modulus of poly(GMA-*co*-PEGMA950) cured with sonication as measured via NIC. Samples were crosslinked with a 1:1 molar ratio of thiol to epoxy and at a DP of 100, 150, or 200 and measured 60 s post sonication and after two weeks.

low equilibrium modulus implies the presence of unreacted crosslinks. With the same number of crosslinks possible in MEMA, PEGMA500, and PEGMA950 samples, and taking the equilibrium modulus of the MEMA polymer in **Figure 1c**, PEGMA500 and PEGMA950 can be inferred to be have a lower crosslinking density due to the protective effects of the polyether chains. This led us to believe that 950 g/mol shielding groups are most effective at creating a steric barrier to reaction, preventing crosslinking between adjacent polymers and resulting in lower final G' values.

| Name | Target DP | Feed ratio | Actual DP | Actual ratio |
|-------------------------|-----------|------------|-----------|--------------|
| 50:50 GMA:MEMA | 50 | 1:1 | 73 | 55:45 |
| 50:50 GMA:PEGMA500 | 50 | 1:1 | 122 | 51:49 |
| 50:50 GMA:PEGMA950 | 50 | 1:1 | 91 | 56:44 |
| 60:40 GMA:PEGMA950 | 50 | 60:40 | 102 | 62:38 |
| 70:30 GMA:PEGMA950 | 50 | 70:30 | 87 | 72:28 |
| 30:70 GMA:PEGMA500 | 50 | 30:70 | 76 | 30:70 |
| 60:40 GMA:PEGMA950 | 50 | 60:40 | 119 | 60:40 |
| 70:30 GMA:PEGMA500 | 50 | 70:30 | 95 | 68:32 |
| 60:40 GMA:MEMA | 50 | 60:40 | 134 | 60:40 |
| 70:30 GMA:MEMA | 50 | 70:30 | 140 | 70:30 |
| 50:50 GMA:PEGMA950 25DP | 25 | 1:1 | 34 | 1:1 |
| 50:50 GMA:PEGMA950 50DP | 50 | 1:1 | 61 | 54:46 |
| 50:50 | 100 | 1:1 | 93 | 1:1 |

| | | | | |
|--------------------|-------|-----|-----|-------|
| GMA:PEGMA950 | 100DP | 1:1 | 130 | 52:48 |
| 50:50 GMA:PEGMA950 | 150DP | 1:1 | 191 | 57:43 |
| 50:50 GMA:PEGMA950 | 200DP | 1:1 | | |

Controlling gel time through shield graft density

We next aimed to determine the minimum molar ratio of shielding groups necessary to prevent spontaneous crosslinking by varying the ratio of GMA:PEGMA (**Figure 2a**). We expected that high contents of shielding monomer would entirely inhibit gelation over the measurement time, eventually prohibiting crosslinking even under force. To assess the minimum molar ratio necessary for preventing gelation without applied mechanical stimulus, the mole percent of PEGMA950 (~20 repeat units) and PEGMA500 (~10 repeat units) shielding monomers within each polymer chain was varied from 30 to 50 mol%. Variations in mole percent of MEMA copolymers was assessed as a negative control. The total concentration of epoxides in solution remained constant at 1 M.

In the presence of EDA or EDT with shielding group concentrations at mol 50% (PEGMA950), a negligible increase in G' was seen; at 40%, a very slow increase in G' with a final value on the order of 10^3 Pa was demonstrated; and at 30%, a rapid increase in G' with a final G' of 10^4 Pa (**Figure 2b-c**). At higher shielding monomer percentages, gelation was entirely inhibited over the measurement time, even with the quick crosslinking EDT. In both the thiol and amine cases, the trend toward decreasing gel time with increasing PEGMA950 content is the same.

Next, polymers with PEGMA500 shielding units (~10 repeat units) were varied from 30 to 70 mol% shielding monomer content while keeping the total epoxide group concentration in solution constant at 1 M (**Figure 2d**) with EDA. When the shielding group concentration was 30 and 40 mol %, the material crosslinks rapidly and reaches final G' values on the order of 10^5 Pa. At 50% concentration of shielding groups, the material reaches a lower final

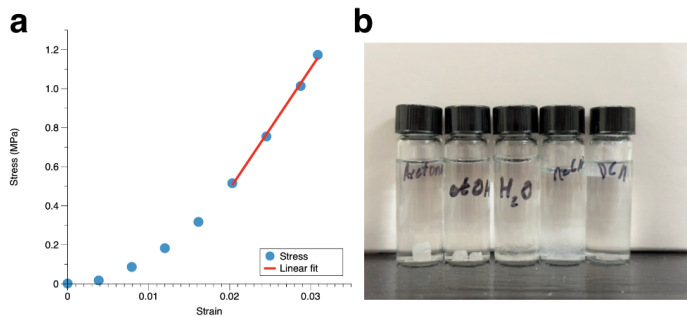


Figure 4. Shielded copolymers create ultrahard and durable materials. a. Compression modulus of a fully cured poly(GMA-co-PEGMA2000) with 1:1 molar ratio of monomers. Elastic modulus is calculated by taking the slope during the linear portion of the stress-strain curve. Red line shows the linear best fit through four points. b. Fully cured poly(GMA-co-PEGMA2000) gels immersed into acetone, ethanol, water, acetonitrile, and dichloromethane.

modulus on the order of 10^4 Pa. At the maximum tested 70% molar ratio of shielding group to reactive group, the shielded polymers still form a gel, but do not attain an equilibrium modulus during the experimental timeframe. The PEGMA500 shielding groups do not provide a sufficient steric barrier to reaction but do provide some hindrance to reaction evidenced by the decreased final modulus values compared to control samples.

Finally, polymers with one repeat unit pendent chains (MEMA) were varied between 30 and 50 mol% control monomer and reacted in the presence of EDA. Increasing the control monomer ratio from 30 to 50% slightly decreased to rate at which the material crosslinked and the final modulus, from 10^5 Pa at 30 and 40 mol% control monomer to just above 10^4 Pa at 50 mol% control monomer (Figure 2e). As expected, the small size of the MEMA comonomer did not contribute significantly to suppressing the crosslinking kinetics of the crosslinking polymers.

At low ratios of shielding monomer to reactive monomer, there are statistically likely to be more stretches of reactive monomer with no steric effects to prevent them from crosslinking, as well as increased backbone flexibility. At high ratios of shielding monomer to reactive monomer, there are far fewer reactive monomer sequences as well as a straighter backbone due to pendent chains preventing backbone flexing. In summary, only the poly(GMA-co-PEGMA950) compositions achieved this with a high degree of shielding. Gelation was completely inhibited at a 1:1 ratio of reactive to shielding groups. This composition was selected as the most promising candidate for force-activated gelation.

Force-induced gelation of shielded copolymers

We hypothesized sonication would be a facile method to mechanically induce gelation of shielded polymer.

Sonication can achieve enormous strain rates approaching 10^8 s⁻¹³⁵. This enormous strain rate arises from cavitations introduced during ultrasonic irradiation, nearly instantaneously creating and destroying microscopic bubbles that in turn create pressure gradients able to apply force through fast solvent flows to polymers of sufficient size. The force accumulated along the polymer backbone result in overstretched regions, which is what is generally accepted to drive conventional mechanochemical reactions³⁶.

Crosslinking of shielded polymers induced *via* sonication was assessed at DP of 25 to 200 monomer units per chain (Figure 3a). Each polymer sample was prepared at 1 M epoxide group concentration and reacted with EDT catalyzed by LiOH. Utilizing an ultrasonic probe immersed in polymer solutions, samples were subjected to ultrasonic waves for 5 s at a time, with 10 s of pause in between to prevent probe overheating. All conditions have delayed gelation at static conditions, allowing for the characterization of faster crosslinking with induced strain. At DP equal or greater to 100, samples gelled within 60 s of sonication time. At 100 DP, we observed a two order of magnitude decrease in gelation time when comparing unperturbed samples with sonicated samples. Samples of DP 150 and 200 gelled more rapidly, within 30 and 20 seconds of sonication time, respectively. Poly(GMA-co-PEGMA950) of lower DP (25 and 50) did not show any strain responsiveness, and the solution boiled before any gelation or viscosity change was observed due to the heat generated by the ultrasonic probe, reaching a temperature of 56°C measured through an IR thermometer, at which point the solution began to boil while sonication was being applied. Counterintuitively, the heat generated by sonication is counterproductive to gelation of this system, possibly due to changes in the conformation of PEGMA shielding groups at higher temperatures (Figure S11). It is well understood that PEGMA copolymers have a lower critical solution temperature in water that is dependent on the polyether length and the ionic strength of the environment³⁷, but it is not clear that this behavior extends into aprotic organic solvents. Gelation time under static conditions decreased as a function of DP like sonicated samples but showed a leveling off after 150 DP unlike the sonicated samples. This decrease in gel time is likely due to the longer backbone lengths of the polymers beginning closer to the percolation threshold for gelation, resulting in fewer epoxide-thiol reactions needing to take place to form a volume spanning elastic path and a shorter time to the critical gel^{38,39}.

It has been shown that polymers of sufficient molecular weight are sensitive to shear forces. The large size of polymers results in restriction of bond angle conformers available due to chain and bond torsional strain, meaning polymers can accumulate force along their backbone as

entropic potential energy⁴⁰⁻⁴³. High molecular weight polymers undergo chain scission in response to strong shear forces generating two distinct carbon-centered radicals^{44,45}. These sufficiently strong shear forces result in overstretched segments of polymer adjacent to the chain center, generating a tensile force that drives mechanochemical reactions³⁶. The chain scission rate increases with molecular weight⁴⁶. This molecular weight dependence is more accurately described as a polymer length dependence⁴⁷. It follows that shielded poly(GMA-*co*-PEGMA950) of sufficient DP is more easily influenced by shear forces in solution if the chain length is long enough, surpassing at least 100 units in length. The increased DP of the polymer also increases the viscosity of the sample. Prior literature has shown that highly viscous media decreases the effectiveness of ultrasonic micromixing⁴⁸, making it less likely that the dependence of gel time on DP is a result of mixing phenomena. This study does not elucidate the mechanism for this system's strain sensitivity. It is not clear what aspect of crosslinking is sped up by the application of ultrasound, the addition of EDT to polymer or the addition of polymer+EDT to another polymer. Future studies using mono-thiols functionalized with UV tags would shed light on the precise molecular mechanism of strain-sensitive crosslinking.

Cavitation rheology was used to assess post-gelation elastic moduli of gels formed *via* sonication (**Figure 3b**). NIC has previously been shown to be effective at extracting elastic modulus information from soft materials²⁷. Sonicated samples were measured to have an elastic modulus near 1 kPa for samples starting at 100 DP, and 20 kPa for samples between 150 and 200 DP as measured by NIC. After a week of resting in a sealed tube to allow for residual epoxides to be consumed by thiols, the modulus of each sample increased to an average of 20 kPa for samples starting at 100 DP and 60 kPa for samples starting at 150 to 200 DP. The final modulus for 150 and 200 DP polymers had a wide range, varying from 30 to 170 kPa. This variance is likely error from cavitation rheology, which tends to have higher variance for samples with higher elastic moduli^{49,50}. The modulus derived from NIC shows polymers shielded with PEGMA950 cure into relatively weak materials.

Ultrahard materials from shielded copolymers

Conventional epoxy resins and composites can attain G' values approaching and surpassing 10^9 Pa^{51,52}. Choosing this value as a benchmark for comparison, we formulated poly(GMA-*co*-PEGMA2000) copolymers at a 1:1 monomer ratio and 670 DP. The extremely long shielding group and long DP were chosen to provide a material that had both maximum latency and sensitivity to ultrasound. After sonicating these samples and leaving them to cure for 48 hr, the polymer crosslinked into an opaque white solid.

Samples were prepared as 5x4 mm cylinders, and their moduli were assessed on a rheometer *via* compression with a 4 mm diameter plate. An elastic modulus value of 62 MPa was extracted from the resultant stress-strain curve (**Figure 4a**), approaching that of conventional epoxy materials. Immersing gels of this copolymer into acetone and ethanol showed no visible change in the material, but in MeCN, DCM, and water the gels crumbled into insoluble chunks (**Figure 4b**), leading us to conclude that the material's strength comes from a combination of epoxide-thiol covalent crosslinks and PEG side chain crystallization. It is well known that graft copolymers with crystallizable side chains will form crystal domains^{53,54}. Using DSC we were able to measure a melting temperature for a cured GMA:PEGMA2000 sample, confirming the material is partially crystallized (**Figure S12**). Using a steric shielding approach, we created an ultrahard material through an unexpected combination of crystallinity and covalent bonding.

Conclusion

We synthesized novel strain-sensitive shielded polymers containing both reactive epoxides and molecular shields. These shielding PEG chains provide a steric barrier to an otherwise powerful and efficient crosslinking reaction between amines or thiols and epoxides. This approach to creating strain sensitive materials provides a facile route to creating strain responsive coatings and adhesives, using well-known and commercially available monomers. Through this we demonstrated, for the first time, a liquid-to-solid transition accelerated under force using shielded reactive polymers. We showed that force stimulated gelation could be achieved with ultrasound. We further showed that steric shielding can create ultrahard materials. Suppressed gelation without force, combined with ultrasound sensitivity, make this polymer an ideal candidate for an adhesive in a heat or light sensitive application.

Supporting Information

¹H NMR spectra, temperature control rheology, DSC thermogram.

Video S1, example sonication setup.

Author Information

Corresponding Authors

Shelly Peyton — Department of Chemical Engineering, University of Massachusetts Amherst, Amherst, Massachusetts 01003, United States; **Email:** speyton@umass.edu

John Klier — Department of Chemical Engineering, Oklahoma University, Norman, Oklahoma 73019, United States; **Email:** klier@ou.edu

Authors

Adrian A. Lorenzana — Department of Chemical Engineering, University of Massachusetts Amherst, Amherst, Massachusetts 01003, United States; **Email:** alorenzana@umass.edu

Hsu Shwe Yee Naing — Department of Chemical Engineering, University of Massachusetts Amherst, Amherst, Massachusetts 01003, United States; **Email:** hnaing@umass.edu

Jichao Song — Department of Chemical Engineering, University of Massachusetts Amherst, Amherst, Massachusetts 01003, United States; **Email:** jichaosong@umass.edu

Jessica D. Schiffman — Department of Chemical Engineering, University of Massachusetts Amherst, Amherst, Massachusetts 01003, United States; **Email:** schiffman@umass.edu

1. Rimmer, S. *et al.* Epithelialization of hydrogels achieved by amine functionalization and co-culture with stromal cells. *Biomaterials* **28**, 5319–5331 (2007).
2. Villani, M., Deshmukh, Y. S., Camlibel, C., Esteves, A. C. C. & With, G. D. Superior relaxation of stresses and self-healing behavior of epoxy-amine coatings. *RSC Advances* **6**, 245–259 (2015).
3. Wang, S., Shuai, L., Saha, B., Vlachos, D. G. & Epps, T. H. From Tree to Tape: Direct Synthesis of Pressure Sensitive Adhesives from Depolymerized Raw Lignocellulosic Biomass. *ACS Central Science* **4**, 701–708 (2018).
4. Frounchi, M., Dadbin, S. & Panahinia, F. Comparison between electron-beam and chemical crosslinking of silicone rubber. *Nuclear Instruments and Methods in Physics Research Section B: Beam Interactions with Materials and Atoms* **243**, 354–358 (2006).
5. Brown, A. E. X., Litvinov, R. I., Discher, D. E., Purohit, P. K. & Weisel, J. W. Multiscale Mechanics of Fibrin Polymer: Gel Stretching with Protein Unfolding and Loss of Water. *Science* **325**, 741–744 (2009).
6. Bu, T., Wang, H.-C. E. & Li, H. Single Molecule Force Spectroscopy Reveals Critical Roles of Hydrophobic Core Packing in Determining the Mechanical Stability of Protein GB1. *Langmuir* **28**, 12319–12325 (2012).
7. Gee, E. P. S., Ingber, D. E. & Stultz, C. M.

Acknowledgements

We kindly thank Dr. Carey Dougan help with cavitation rheology, experimental setup, and instruction. We thank Dr. H. Henning Winter for interpretation of rheological data. We thank Dr. Jessica D. Schiffman and Dr. H. Henning Winter for use of their rheometer. We thank the Polymer Science and Engineering department and Dr. Weiguo Hu for training and use of the NMR facilities. We thank the Crosby Lab for use of their custom LabView software. We thank Sally Prasch at the University of Massachusetts Amherst Glassblowing Laboratory for the custom glassware. We thank Dr. Nathan Richbourg, Dr. Megan Wancura, and Auggie Wirasaputra for manuscript editing. This research was supported by a grant from the Army Research Office (W911NF1910388) to S.R.P. and J.K. A.L was supported by an NIH funded Chemistry Biology Interface Fellowship (T32 GM008515 and T32 GM139789), and a Spaulding-Smith Fellowship from the UMass Amherst Graduate School.

References

1. Fibronectin Unfolding Revisited: Modeling Cell Traction-Mediated Unfolding of the Tenth Type-III Repeat. *PLOS ONE* **3**, e2373 (2008).
2. Smith, M. L. *et al.* Force-Induced Unfolding of Fibronectin in the Extracellular Matrix of Living Cells. *PLOS Biology* **5**, e268 (2007).
3. Oberhauser, A. F., Badilla-Fernandez, C., Carrion-Vazquez, M. & Fernandez, J. M. The Mechanical Hierarchies of Fibronectin Observed with Single-molecule AFM. *Journal of Molecular Biology* **319**, 433–447 (2002).
4. Kuijpers, M. W. A., Iedema, P. D., Kemmere, M. F. & Keurentjes, J. T. F. The mechanism of cavitation-induced polymer scission; experimental and computational verification. *Polymer* **45**, 6461–6467 (2004).
5. Tran, Y. H., Rasmussen, M. J., Emrick, T., Klier, J. & Peyton, S. R. Strain-stiffening gels based on latent crosslinking. *Soft Matter* **13**, 9007–9014 (2017).
6. Sonu, K. P. *et al.* Strain-Stiffening Hydrogels with Dynamic, Secondary Cross-Linking. *Langmuir* **39**, 2659–2666 (2023).
7. Ramirez, A. L. B. *et al.* Mechanochemical strengthening of a synthetic polymer in response to typically destructive shear forces. *Nature Chemistry* **5**, 757–761 (2013).
8. Lenhardt, J. M., Black Ramirez, A. L., Lee, B., Kouznetsova, T. B. & Craig, S. L. Mechanistic Insights into the Sonochemical Activation of

Multimechanophore Cyclopropanated Polybutadiene Polymers. *Macromolecules* **48**, 6396–6403 (2015).

15. Hickenboth, C. R. *et al.* Biasing reaction pathways with mechanical force. *Nature* **446**, 423–427 (2007).
16. Yu, X. *et al.* Sonication-triggered instantaneous gel-to-gel transformation. *Chemistry* **16**, 9099–9106 (2010).
17. Vidil, T., Tournilhac, F., Musso, S., Robisson, A. & Leibler, L. Control of reactions and network structures of epoxy thermosets. *Topical Volume on Polymer chemistry* **62**, 126–179 (2016).
18. Izunobi, J. U. & Higginbotham, C. L. Polymer Molecular Weight Analysis by ^1H NMR Spectroscopy. *Journal of Chemical Education* **88**, 1098–1104 (2011).
19. Keddie, D. J., Moad, G., Rizzardo, E. & Thang, S. H. RAFT Agent Design and Synthesis. *Macromolecules* **45**, 5321–5342 (2012).
20. Ehlers, J.-E. *et al.* Theoretical Study on Mechanisms of the Epoxy–Amine Curing Reaction. *Macromolecules* **40**, 4370–4377 (2007).
21. Gadwal, I., Stuparu, M. C. & Khan, A. Homopolymer bifunctionalization through sequential thiol-epoxy and esterification reactions: an optimization, quantification, and structural elucidation study. *Polymer Chemistry* **6**, 1393–1404 (2015).
22. Winter, H. H. & Chambon, F. Analysis of Linear Viscoelasticity of a Crosslinking Polymer at the Gel Point. *Journal of Rheology* **30**, 367–382 (1986).
23. Chambon, F. & Winter, H. H. Stopping of crosslinking reaction in a PDMS polymer at the gel point. *Polymer Bulletin* **13**, (1985).
24. Chambon, F. & Winter, H. H. Linear Viscoelasticity at the Gel Point of a Crosslinking PDMS with Imbalanced Stoichiometry. *Journal of Rheology* **31**, 683–697 (1987).
25. Poh, L., Narimissa, E., Wagner, M. H. & Winter, H. H. Interactive Shear and Extensional Rheology-25 years of IRIS Software. *Rheologica Acta* **61**, 259–269 (2022).
26. Kong, Y. & Hay, J. N. The measurement of the crystallinity of polymers by DSC. *Polymer* **43**, 3873–3878 (2002).
27. Dougan, C. E. *et al.* Cavitation induced fracture of intact brain tissue. *Biophysical Journal* **121**, 2721–2729 (2022).
28. Barney, C. W. *et al.* Cavitation in soft matter. *Proceedings of the National Academy of Sciences* **117**, 9157–9165 (2020).
29. Li, Z. *et al.* Bottlebrush polymers: From controlled synthesis, self-assembly, properties to applications. *Progress in Polymer Science* **116**, 101387 (2021).
30. T. Nguyen, L.-T., Talha Gokmen, M. & Prez, F. E. D. Kinetic comparison of 13 homogeneous thiol–X reactions. *Polymer Chemistry* **4**, 5527–5536 (2013).
31. Flory, P. J. Molecular Size Distribution in Three Dimensional Polymers. I. Gelation1. *Journal of the American Chemical Society* **63**, 3083–3090 (1941).
32. Flory, P. J. *Principles of Polymer Chemistry* (Cornell University Press, 1953).
33. Ferry, J. D. *Viscoelastic Properties of Polymers* (John Wiley & Sons, 1980).
34. Kulicke, W. M. & Nottelmann, H. Structure and Swelling of Some Synthetic, Semisynthetic, and Biopolymer Hydrogels. in *Polymers in Aqueous Media* 15–44 (American Chemical Society, 1989).
35. Hennrich, F. *et al.* The Mechanism of Cavitation-Induced Scission of Single-Walled Carbon Nanotubes. *The Journal of Physical Chemistry B* **111**, 1932–1937 (2007).
36. O’Neill, R. T. & Boulatov, R. Experimental quantitation of molecular conditions responsible for flow-induced polymer mechanochemistry. *Nature Chemistry* **15**, 1214–1223 (2023).
37. Lutz, J.-F. & Hoth, A. Preparation of Ideal PEG Analogues with a Tunable Thermosensitivity by Controlled Radical Copolymerization of 2-(2-Methoxyethoxy)ethyl Methacrylate and Oligo(ethylene glycol) Methacrylate. *Macromolecules* **39**, 893–896 (2006).
38. Daoud, M. Viscoelasticity near the Sol–Gel Transition. *Macromolecules* **33**, 3019–3022 (2000).
39. Winter, H. H. Gel Point. in *Encyclopedia of Polymer Science and Technology* 1–15 (John Wiley & Sons, Ltd, 2016).
40. Wang, K., Pang, X. & Cui, S. Inherent Stretching Elasticity of a Single Polymer Chain with a Carbon,–Carbon Backbone. *Langmuir* **29**, 4315–4319 (2013).
41. Hermes, M. & Boulatov, R. The Entropic and Enthalpic Contributions to Force-Dependent Dissociation Kinetics of the Pyrophosphate Bond.

Journal of the American Chemical Society **133**, 20044–20047 (2011).

42. Shi, W. *et al.* Toward understanding the effect of substitutes and solvents on entropic and enthalpic elasticity of single dendronized copolymers. *Polymer* **47**, 2499–2504 (2006).

43. Cui, S., Yu, Y. & Lin, Z. Modeling single chain elasticity of single-stranded DNA: A comparison of three models. *Polymer* **50**, 930–935 (2009).

44. Caruso, M. M. *et al.* Mechanically-Induced Chemical Changes in Polymeric Materials. *Chemical Reviews* **109**, 5755–5798 (2009).

45. Beyer, M. K. & Clausen-Schaumann, H. Mechanochemistry: the mechanical activation of covalent bonds. *Chem Rev* **105**, 2921–2948 (2005).

46. Madras, G., Kumar, S. & Chattopadhyay, S. Continuous distribution kinetics for ultrasonic degradation of polymers. *Polymer Degradation and Stability* **69**, 73–78 (2000).

47. May, P. A., Munaretto, N. F., Hamoy, M. B., Robb, M. J. & Moore, J. S. Is Molecular Weight or Degree of Polymerization a Better Descriptor of Ultrasound-Induced Mechanochemical Transduction? *ACS Macro Letters* **5**, 177–180 (2016).

48. Monnier, H., Wilhelm, A. M. & Delmas, H. Influence of ultrasound on mixing on the molecular scale for water and viscous liquids. *Ultrasonics Sonochemistry* **6**, 67–74 (1999).

49. Zimberlin, J. A., Sanabria-DeLong, N., Tew, G. N. & Crosby, A. J. Cavitation rheology for soft materials. *Soft Matter* **3**, 763–767 (2007).

50. Barney, C. W., Zheng, Y., Wu, S., Cai, S. & Crosby, A. J. Residual strain effects in needle-induced cavitation. *Soft Matter* **15**, 7390–7397 (2019).

51. Baral, N., Davies, P., Baley, C. & Bigourdan, B. Delamination behaviour of very high modulus carbon/epoxy marine composites. *Composites Science and Technology* **68**, 995–1007 (2008).

52. Mąka, H., Spycharj, T. & Zenker, M. High performance epoxy composites cured with ionic liquids. *Journal of Industrial and Engineering Chemistry* **31**, 192–198 (2015).

53. Takeshita, H., Sasagawa, G., Takenaka, K., Miya, M. & Shiomi, T. Crystallization of graft copolymers 1. Graft chains miscible with main chains. *Polymer Journal* **42**, 482–488 (2010).

54. Inomata, K., Nakanishi, E., Sakane, Y., Koike, M. & Nose, T. Side-chain crystallization behavior of graft copolymers consisting of amorphous main chain and crystalline side chains: Poly(methyl methacrylate)-graft-poly(ethylene glycol) and poly(methyl acrylate)-graft-poly(ethylene glycol). *Journal of Polymer Science Part B: Polymer Physics* **43**, 79–86 (2005).